



# Experimental Identification and Hybrid PID-Fuzzy Position Control of Continuum Robotic Arms

A. Parvaresh<sup>a</sup>, S. A. A. Moosavian<sup>a,\*</sup>

<sup>a</sup> Center of Excellence in Robotics and Control, Advanced Robotics & Automated Systems (ARAS) Laboratory  
Faculty of Mechanical Engineering, K. N. Toosi University of Technology

## ARTICLE INFO

### Article history:

Received: 1 October 2019  
Received in revised form: 15 February 2020  
Accepted: 3 March 2020

### Keywords:

Continuum robotic arm  
System identification  
Fuzzy-PID controller  
Position control

## ABSTRACT

Continuum robotic arms that are inspired from nature, have many advantages compared to traditional robots, which motivate researchers in this field. Dynamic modeling and controlling these robots are challenging subjects due to complicated nonlinearities and considerable uncertainties existing in these structures. In this paper, first a dynamic three-dimensional model of the continuum robotic arm is developed as a black-box model through system identification method. The validity of the obtained model is confirmed by the experimental data. Then, by using the obtained model, a hybrid PID-fuzzy controller, which is considered as a model-free controller and does not require the exact model of the system is employed for controlling the position of the end-effector. Finally, obtained results and the performance of the controller in reaching to different positions of the workspace, either trained or not, is discussed.

## 1. Introduction

Continuum robotic arms are the class of robots that are inspired from the nature and inherent capabilities of creatures such as elephant's trunk, octopus arms, squid tentacles and etc. As defined in [1], a continuum manipulator is a continuously bending, infinite-degree of-freedom robot with an elastic structure. These manipulators can handle the difficulties encountered in the rigid robotics area, such as problems in the unstructured environments, grasping un-programmed objects, undesired collision with the obstacles in the environment, and higher energy consumption by their inherent capabilities and can be constructed with larger workspace, higher operational speed, smaller actuators, higher maneuverability, and safer operation [2].

Tendon-driven continuum manipulators are one of the most common continuum manipulators according to their amazing advantages in generation of higher forces, realizable design and structure, and external actuation, which made them smaller and safer in comparison with the other types of continuum manipulator such as concentric tubes. These manipulator have an elastic backbone, the configuration of which can be controlled by a set of tendons that are fixed parallel with respect to the tendons [3]. These types are mostly used in minimally invasive surgeries (MIS) [4], under-water [5] and space applications [6].

Kinematic model relates the variables in the configuration space to the variables in task and actuator spaces [7]. Different methods have been proposed for kinematic modeling of continuum robots. In [8], by assuming a constant curvature for two dimensional

\*. corresponding author: K. N. Toosi University of Technology, Tehran, Iran,  
Email address: moosavian@kntu.ac

backbone of the robot, kinematics of the robot was modeled using D-H approach. In [9], the same procedure was performed for a three-dimensional multi-section robot. Instead of using a circular arc for whole body, Hannan and Walker [9], used piecewise circular arcs for each section of the robot, in which the curvature was different in each section and then the closed-form solutions were obtained for the kinematics of the robot. For more exact solution, Dehgani and Moosavian [10] used Cosserat rod theory for static modeling of the continuum robotic arm. Due to the complexity of extracting closed-form static and dynamic models, In [11], Yip et al, used empirical Jacobian method for extracting the dynamics of the robot for using in control applications. Renda et al, [12] modified the continuum Cosserat approach, which can be discretized in a finite number of sections and degrees of freedom. In this model, torsion and shears strains were also considered and the dynamic model was obtained.

Controlling Continuum robotic arms involves many challenges according to their under actuated structure and infinite degrees of freedom, non-accurate modeling, nonlinearity, uncertainty and lack of direct relationship between the actuation variables and configuration variables. Therefore, investigations in the field of continuum robot control are in the first steps and many improvements should be conducted [13]. Control strategies can be classified into three main groups: model-based controllers, which rely on the analytical methods, model-free controllers, which uses intelligent techniques or empirical methods, and hybrid controllers, which combines the both methods for designing the controller [14].

Model-based static controllers are the most studied strategies according to the simplicity and availability of the static models. In [15], a closed-loop controller in the task space was proposed for controlling the end-effector of a tendon-driven continuum robot using D-H kinematic model. In [16], a controller in the configuration space was proposed. In this method, the information about the configuration of the robot was obtained using external sensory information and the stability of the controller proved by Lyapunov's direct method. In [17], a closed-loop position-feedback kinematic controller was proposed for the constant-curvature based model of a tendon-driven robot, and a quadratic programming algorithm is incorporated into the controller.

According to the fact that model-free static controllers do not require any analytical models, more complex kinematic models can be developed according to the sampled data. These techniques shows better performance in highly nonlinear, non-uniform, and influenced by gravity systems and are relatively new field[14]. In [11], a closed-loop controller was proposed using an optimal control strategy for a tendon-driven

continuum robot based on the empirical estimation of the kinematic Jacobian matrix. This controller did not rely on model and could be used in constrained environments. In [18], the same approach was extended for force/position hybrid control, in which the stiffness matrix was also computed empirically. In [19], a learning approach was used for modeling and control of a continuum robot. In this research, neural network model was used for learning the kinematics and it was validated experimentally, then this model was used for controlling the continuum robot, and its real-time implementation allowed controlling of the end-effector position [1].

PID controllers are classified as model-free controllers and provide a relatively simple structure along with robust performance. The performances of these controllers are highly dependent on the selection of PID gains, which is difficult procedure if some uncertainties exist. Fuzzy logic-based controllers employ approximate reasoning as the decision making process in humans. These controllers are also do not rely on the mathematical model of the plant.

To profit the advantages of these two types of controllers, hybrid PID-Fuzzy controllers are proposed. These controllers have self-tuning features and are applicable in nonlinear time-varying systems with uncertainties. The gains of PID in these hybrid controllers are tuned by incremental fuzzy logic controller.

In this paper, due to the mentioned problems in modeling of the continuum robots analytically, we aim to model the robot through the system identification of the robot, so solving the complicated equations is eliminated and a three dimensional model of the robot is developed using NARX (nonlinear autoregressive model with exogenous input) model. The validity of the obtained model is confirmed by the experimental data. Despite the model-based controllers, which require analytical model of the robot, in order to control the position of the end-effector with the proposed model, a PID controller, which is considered as a model-free controller and do not require exact model is used and its coefficients are tuned using fuzzy interface system.

The rest of the paper is organized as follows: In section II, the actuation and sensing system of the continuum robot is demonstrated, next, in section III, the modeling procedure of the robot using data-driven system identification is explained and validated. The hybrid control scheme for positioning the end-effector of the continuum arm in the desired position is detailed in section IV. After that, in section V, the results of the robot simulation is provided and finally, section VI is dedicated to the conclusion.

## 2. System description

The continuum robotic arm studied in this paper is a tendon-driven two-section arm with a flexible backbone. By applying the forces to the tendons, the shape and position of the robot can be controlled. This robot is classified as external actuation systems. The schematic and real continuum robotic arm along with the backbone, spacers, guides and tendons are depicted in Fig. 1.

The total length of the robot is 593 millimeters and it is divided into two sections. Each section has three tendons that are fixed parallel with respect to the backbone by spacers in each 3 centimeter distance. The tendons are placed radially with respect to the backbone with the radial space of 120 degrees. In the actuation system, six Dynamixel servo motors (AX-12) are used for applying the force to the tendons and also six load cells are provided for sensing the applied forces. The image processing technique is used to capture the position of the end effector and any other point in the manipulator backbone. Two A4-tech PK7 cameras, which are placed in fixed distances with respect to the continuum structure are used to capture the precise position of the continuum robotic arm. The internal parameters of these cameras are adjustable, so, they are adjusted to enhance the quality and accuracy of the recorded image. Also, several LEDs are implemented on the manipulator body as well as in different corners of the box, in which the system is placed, in order to facilitate the calibration process. Before each run, the system is first calibrated and then the accurate position of the desired point in the body of the manipulator is recorded by the embedded cameras.

The schematic of the systems components and their connection is represented in Fig. 2. In addition, the properties of the system are provided in Table I. As shown in the Figure, first the written code in the Matlab environment is run and the appropriate signals are sent to the microcontroller (PIC32) through RS 232 serial port. Then the position/force commands are sent to the motor; after gathering the data from load cells and cameras, which are considered as the sensing system, the input-output data set is recorded for system identification purposes. After that the model is obtained, the control scheme can be also implemented on the system.

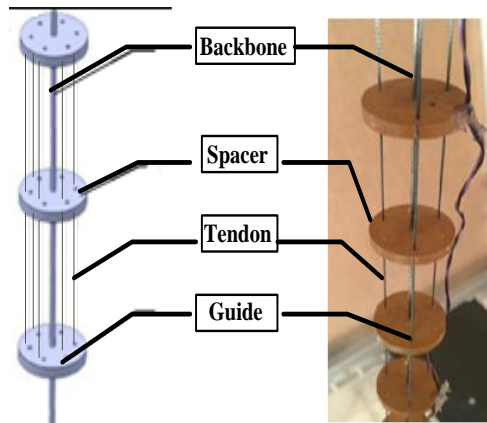


Fig1. The schematic of the Continuum robotic arm

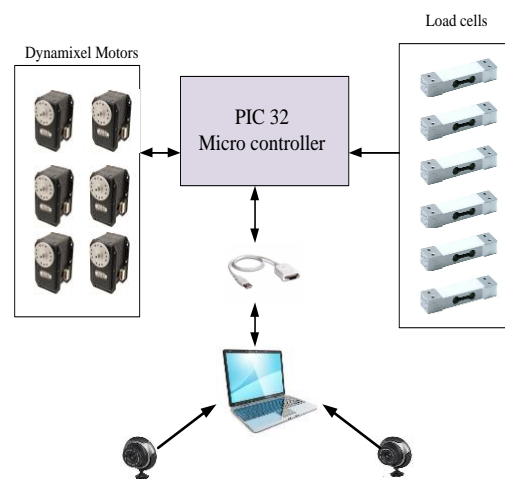


Fig2. Schematic of the cameras, motors, loadcells and their connection to the PC

Table1. Characteristics of the system

|                                      |                        |
|--------------------------------------|------------------------|
| Robot type                           | Tendon-driven backbone |
| Type of actuation                    | Externally             |
| Number of sections                   | 2                      |
| Radial distance of tendons           | 120 degrees            |
| Number of tendon in each section     | 3                      |
| Total degrees of freedom (actuation) | 6                      |
| Total length                         | 593mm                  |
| Backbone Diameter                    | 1mm                    |
| Motor type                           | Dynamixel AX-12        |
| Distance between spacers             | 3 cm                   |
| Backbone Elasticity Modulus          | 203Gpa                 |

### 3. Identification procedure

In this paper, according to the complexities of the dynamic model and the effect of different factors, which cannot be modeled, the system identification (SI) is used to extract a reliable and acceptable model for the robot. The flowchart of this process is explained in Fig. 3. According to this figure, the first step is to determine the excitation signal, and gathering a set of input-output data for training the model. Then the identification is conducted by selecting an appropriate structure and parameters; after that the system is estimated, the validity of the model can be verified by comparing the obtained results from the plant with the collected experimental data.

#### 3.1. Excitation signals

One of the most important steps in system identification is the design of suitable excitation signals in order to gather identification data-sets. This feature is of great significance especially in nonlinear identification due to the complexity of the desired system, in which more information is required for modeling. The excitation signals should be chosen with enough care so that the possibility of gathering much information about the system is provided.

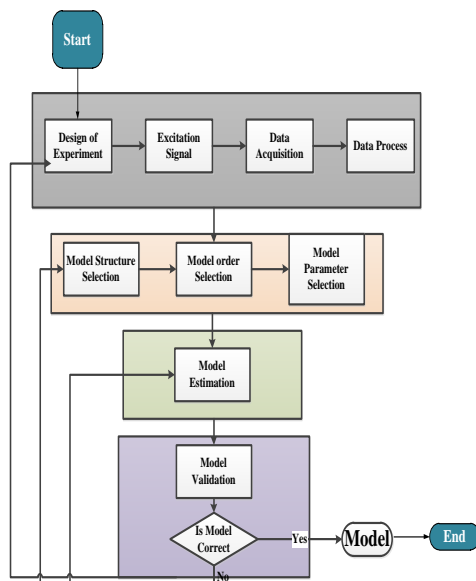


Fig3. The flowchart of system identification

Different excitation signals can be used to excite the system for gathering data, including sine signals, step signals, PBRs and APRBS signals, etc. In excitation with sine signals, the information is collected in a particular frequency and the model quality would be

excellent in the selected frequency. So, if the model is to be used in particular frequency, the combination of sine waves is the best selection for the excitation signal. Therefore, as the studied robot is used in particular frequencies, in this research, we use Sine signal with different frequencies and amplitudes as depicted in Fig. 4 and determined by Eq. 1 .

$$u = \sum_{i=1}^n A_i \sin(\omega_i t) \quad (1)$$

In this equation, u is the excitation signal,  $A_i$  is the amplitude of sine signal;  $\omega_i$  is the sampling frequency and t is the time. Sampling frequency should be selected considering that even the small variations in the system output can be captured. In addition, the amplitudes should be chosen to cover all the feasible workspace of the system. These excitation signals are applied to the servomotors as inputs, which are transformed to the continuum manipulator using RS 323 cable, and then, image processing system, provides the outputs

#### 3.2. Data acquisition

According to the structure of the continuum robot, the positions of the 6 motors are used as inputs as follows:

$$\mathbf{P} = [P_1 \ P_2 \ P_3 \ P_4 \ P_5 \ P_6] \quad (2)$$

And position of the end-effector is used as the outputs of the system:

$$\mathbf{X} = [x_{ee} \ y_{ee} \ z_{ee}]$$

As can be seen in Fig. 4, the input-output data are recorded in the computer. The sampling time is 6s, meaning that in 6 seconds, a complete series of input-output signals are sampled. The sampling time is selected so that the robot's motion can be considered as semi-static and severe vibrations are prevented. It is worth to mention that in designing the system hardware, some filters have been used to eliminate the noises in data, because incorrect reading would result in loss of quality and even, error in modeling the continuum robot. Consequently, in later use of the model, for example in control applications, it may cause the instability of the controller. In Fig. 5 the workspace of the robot corresponding to the excitation signals can be observed. As it is obvious, it is tried to cover all the feasible workspace of the robot for training.

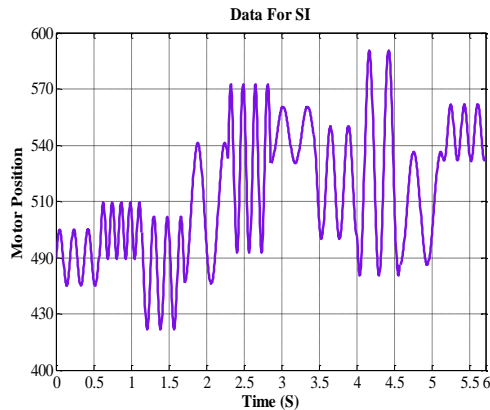


Fig4. Excitation data for system identification

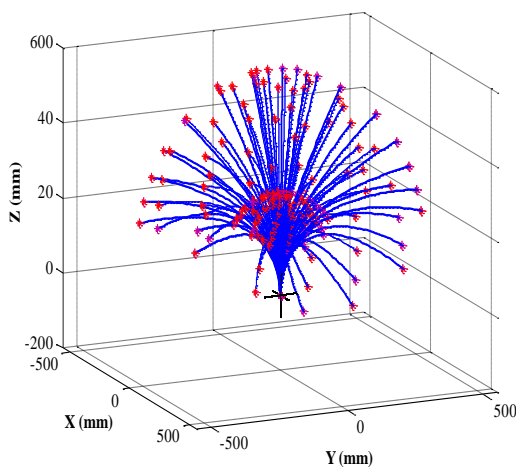


Fig5. The workspace of the continuum robot

### 3.3. Identification structure

In this step, first the type of problem should be specified; it should be clear that the proposed model is to be used for classification, optimization, static or dynamic identification. In addition, the existing constraints such as computational cost, training time, evolution time and so on, should be considered to choose the appropriate structure. Nonlinear autoregressive network with exogenous inputs (NARX) is a recurrent dynamic network, with feedback connections enclosing several layers of the network. Since the continuum robotic arm is a nonlinear system, this structure would be an appropriate choice for the model. The model can be written as follows:

$$\hat{y}(k) = f(\varphi(k)) \quad (3)$$

Where,  $\varphi(k)$  is the regression vector, which contains previous and current process input, previous model outputs, and previous prediction errors.  $f(\cdot)$  is

unknown nonlinear function that can be achieved by implementing the gathered data sets. In fact, the problem of estimating unknown parameters in linear identification is extended to the approximation of nonlinear function of  $f(\cdot)$ .

The detailed procedure is provided in [21]. The model can be approximated by the following equation:

$$y = f\left(\sum_{i=1}^n (w_i x_i + b)\right) \quad (4)$$

In this equation,  $y$  is the output of the system;  $\omega_i$  is the weight for each input, and  $b$  is the bias.

The structure of the system identification procedure is shown in Fig. 6. As shown in this figure, and provided in Table II, the structure is consisted of 18 inputs, 3 outputs and 10 hidden layer. These parameters are selected after several try and errors. It was found that further increasing in the value of the parameters, increase the computational costs considerably; while the accuracy and precision of the model is not changed significantly. The hidden layer poses 10 neurons with hyperbolic tangent sigmoid transfer function and also, a linear transfer function has been used for the output layer. The training function is selected to be Levenberg-Marquette algorithm according to the fact that it is the fastest training algorithm for network of moderate size; in addition, for performance evaluation, mean squared error (MSE) is selected. Finally, for training the CFFNN (cascade feed forward neural network), 2798 data with 0.05 second sample time were employed and for testing the trained model, the validation data sets in the same operating range and number with train data were used.

### 3.4. Model validation

The first step for validating the identified model is to evaluate the model on the training data. Although the performance on training data is necessary, but it is not sufficient. If an acceptable performance is achieved on the train data, then the model should be evaluated by fresh test data. The aim of modeling is to provide a model that performs well on the fresh and unseen test data. So the gathered data should be divided into separate training and testing data sets. In addition, the regression diagram is also plotted for the estimated data. The estimated model is of good quality if the difference between the measured values and predicted values are narrow and close to 1.

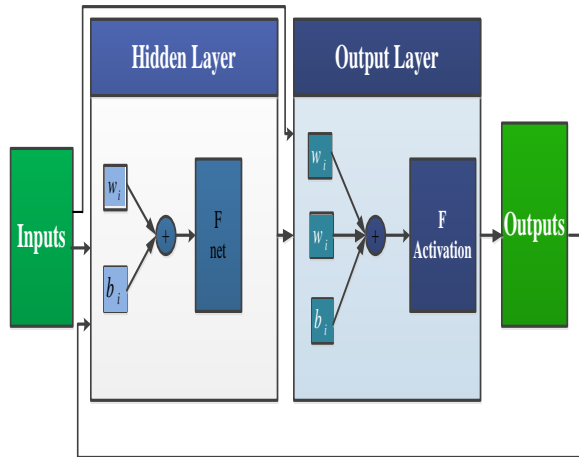


Fig6. Structure of the system identification procedure

Table2. the specification of the training system

| Neural Network Type    | Cascade Feed Forward |
|------------------------|----------------------|
| Inputs                 | 18                   |
| Outputs                | 3                    |
| Hidden Layer           | 1                    |
| Neuron in Hidden Layer | 10                   |
| Iteration              | 250                  |
| Performance Fnc        | MSE                  |
| Train Fnc              | Levenberg-Marquette  |

#### 4. Controller Design

In this section, design of controller for a continuum robotic arm is explained. The NARX model is used as a plant and fuzzy-PID controller is used to control. The control objective of hybrid PID-Fuzzy controller is to produce control signals so that the end effector of manipulator is reached to the desired position in minimum time with good response characteristics. Fuzzy logic systems are widely used in nonlinear and uncertain systems. This system is consisted of fuzzification, rule base, interference engine and defuzzification sections. Fuzzy logic system can be used as a part of adaptive control scheme to tune the parameter of the PID-controller and work in parallel with it. Fuzzy-PID controllers combine the simplicity of PID implementation with the model-free structure of fuzzy controllers to overcome the shortcomings of each control scheme. The schematic of the controlling plant is depicted in Fig. 7, which can be seen with more details in Fig. 8.

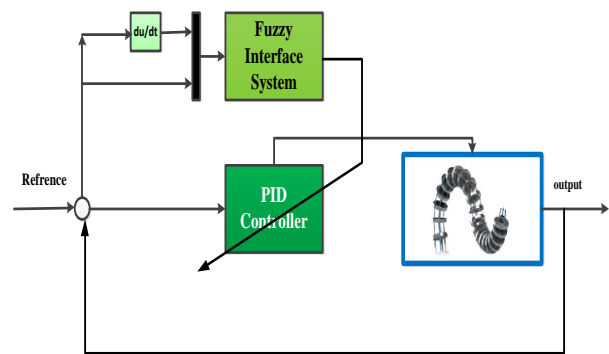


Fig7. The schematic of the controlling system

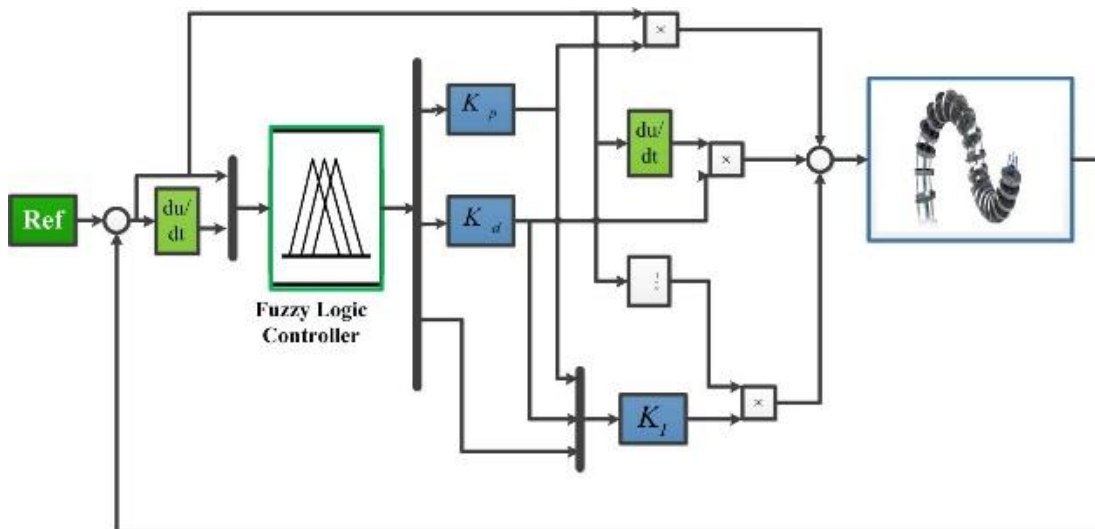


Fig. 8. Implementation of control scheme in Simulink Software

As can be seen from this figure, the reference position of the end-effector ( $x_e, y_e, z_e$ ) is entered to the system and its difference with the real output of the plant is calculated, so, an error signal is generated. This error signal and its derivative are entered to the fuzzy interface system and based on the determined rules; three outputs are generated to tune the coefficients of PID controller. Then the control signals from PID controller are sent to the plant, which is the NARX model of the system. The transfer function of the controller is defined as:

$$G_c = K_p + \frac{K_i}{S} + K_d S \quad (5)$$

$K_p$  is the proportional coefficient,  $K_i$  is the integral coefficient and  $K_d$  is the derivative coefficient. These coefficients are considered to be bounded and normalized as follows:

$$K \in [K_{\min}, K_{\max}]$$

$$\bar{K} = \frac{K - K_{\min}}{K_{\max} - K_{\min}} \quad (6)$$

The control signal is defined as:

$$g(e) = K_p e(t) + K_i \int_0^t e(t) dt + K_d \frac{d}{dt} e(t) \quad (7)$$

In which,  $e(t)$  is the error signal and defined as the difference between the desired reference and system output as:

$$e(t) = x(i)_d - x(i) \quad (8)$$

In which,  $K_i$  is a function of  $\alpha$  and defined as follows:

$$K_i = K_p^2 / \alpha K_d \quad (9)$$

The conventional PID controllers do not provide a reasonable performance since the gains are considered to be constant in all operational conditions; therefore tuning algorithms are needed. Fuzzy algorithm would be an appropriate choice for tuning the PID gains. The membership functions for  $K_p, K_d, \alpha, e(t), \dot{e}(t)$  are defined as triangular membership function in the defined

range, and the rule base is generated based on the previous knowledge of the system from the experiments conducted in the laboratory. The rule-base of the fuzzy system for controller gains ( $K_p, K_d$ ) and  $\alpha$  is depicted in Fig. 9. According to this figure, first the reference values for the x, y and z component of the end-effector is defined and entered to the block labeled as 'x,y,z ref'; then the error signal is generated and entered to the fuzzy logic controller along with its derivative, the output of the fuzzy logic controller generates the tuning parameters for the PID coefficients, which are labeled as  $K_p, K_d$  and  $KI$  in the figure, then its applied to the model of the robot obtained from system identification and the position of the end-effector is obtained.

Table3. Fuzzy Rules for  $K_p$

| $K_p$  | $\dot{e}(t)$ |    |    |    |    |    |    |   |
|--------|--------------|----|----|----|----|----|----|---|
|        | NB           | NM | NS | ZO | PS | PM | PB |   |
| $e(t)$ | NB           | B  | B  | B  | B  | B  | B  | B |
|        | NM           | S  | B  | B  | B  | B  | B  | S |
|        | NS           | S  | S  | B  | B  | B  | S  | S |
|        | ZO           | S  | S  | S  | B  | S  | S  | S |
|        | PS           | S  | S  | B  | B  | B  | S  | S |
|        | PM           | S  | B  | B  | B  | B  | B  | S |
|        | PB           | B  | B  | B  | B  | B  | B  | B |

Table4. Fuzzy Rules for  $K_d$

| $K_d$  | $\dot{e}(t)$ |    |    |    |    |    |    |   |
|--------|--------------|----|----|----|----|----|----|---|
|        | NB           | NM | NS | ZO | PS | PM | PB |   |
| $e(t)$ | NB           | S  | S  | S  | S  | S  | S  | S |
|        | NM           | B  | B  | S  | S  | S  | B  | B |
|        | NS           | B  | B  | B  | S  | B  | B  | B |
|        | ZO           | B  | B  | B  | B  | B  | B  | B |
|        | PS           | B  | B  | B  | S  | B  | B  | B |
|        | PM           | B  | B  | S  | S  | S  | B  | B |
|        | PB           | S  | S  | S  | S  | S  | S  | S |

Table5. Fuzzy Rules for  $\alpha$

| $\alpha$ | $\dot{e}(t)$ |    |    |    |    |    |    |   |
|----------|--------------|----|----|----|----|----|----|---|
|          | NB           | NM | NS | ZO | PS | PM | PB |   |
| $e(t)$   | NB           | 2  | 2  | 2  | 2  | 2  | 2  | 2 |
|          | NM           | 3  | 3  | 2  | 2  | 2  | 3  | 3 |
|          | NS           | 4  | 3  | 3  | 2  | 3  | 3  | 4 |
|          | ZO           | 5  | 4  | 3  | 3  | 3  | 4  | 5 |
|          | PS           | 4  | 3  | 3  | 2  | 3  | 3  | 4 |

|    |   |   |   |   |   |   |   |
|----|---|---|---|---|---|---|---|
| PM | 3 | 3 | 2 | 2 | 2 | 3 | 3 |
| PB | 2 | 2 | 2 | 2 | 2 | 2 | 2 |

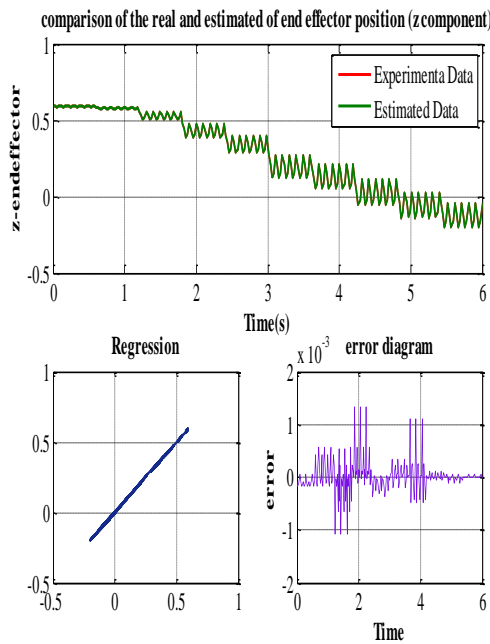


Fig. 9. Fig9. The rule base of the fuzzy system

### 5. Results and Discussions

In this section, the obtained results from the modeling and controlling the continuum robotic arm are provided and discussed. As was previously mentioned, the model of the continuum robotic arm is derived using system identification method through the data obtained from the experiments conducted on the real system.

The below figures (figure 10, 11 and 12) represent the results for modeling the continuum robotic arm through system identification method. It is worth to mention that this method is used, because it is more precise and can be used in the implementation of the control scheme on the real continuum arm, and all the effective parameters are considered; however, in the mathematical modeling of the robot, some factors including friction, uncertainty and ... are not considered due to the high nonlinearity and complexity. So, neglecting these parameters may cause some problems in the implementation on the real system. Additionally, the estimation of the model is performed on-line, which is important in real-time implementation of the controlling scheme in the real robot. However, in the models that are obtained through the mathematical model, especially dynamic models, the real-time implementation is hard to achieve due to the fact that the closed-form solution of the mathematical dynamic model are very complex and therefore time consuming.

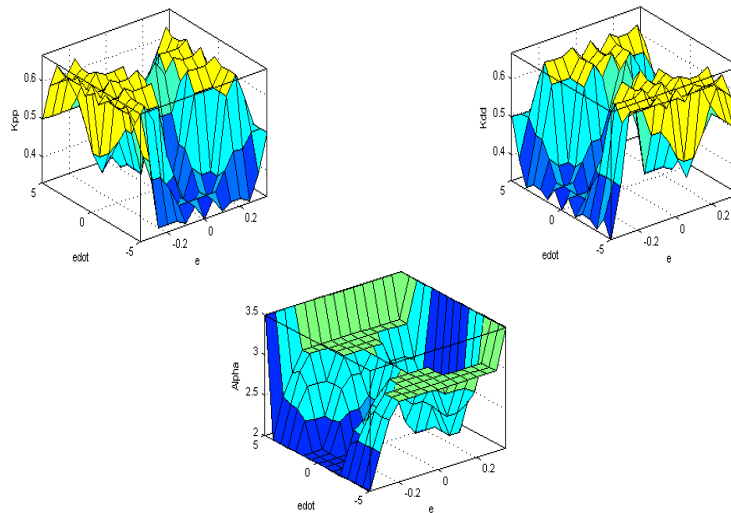


Fig 10. The comparison between the experimental data and estimated data, their regression, and error in the X component of the end effector position



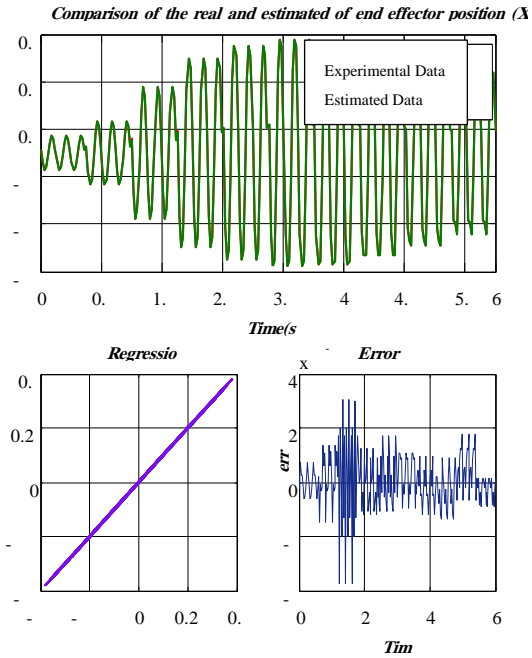


Fig 11. The comparison between the experimental data and estimated data, their regression, and error in the Y component of the end effector position

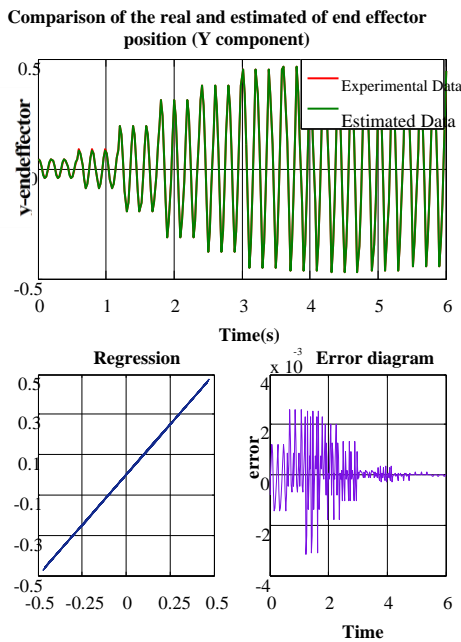


Fig 12. The comparison between the experimental data and estimated data, their regression, and error in the Z component of the end effector position

As can be seen in the above figures, the SI method can model the system acceptably with small error; the error of the estimated data in x, y and z component of the end-effector is in the scale of  $10e-3$ . The next step is to use the obtained model for controlling the robot. A reference in the workspace is

entered to the model of the robot in SIMULINK environment. The aim is that the robot reaches to this position with reasonable properties. Two types of reference are chosen as the inputs of the systems. The first one is considered in the position exactly in the work space of the robot, and the second one is considered in the position far from the trained workspace and the performance of the controller is compared in both states.

The first reference point is considered to be (100,200,550) mm, which is near the trained workspace; the result can be seen in Fig. 13. As can be seen in the figure, the controller shows an acceptable response and converges to the desired position ( $x=100$ mm) without any overshoot after about 10 iterations and no steady state error is observed.

The second reference point is considered to be (200,400,100) mm, which is not trained and far from the trained workspace; the result can be seen in Fig. 14. According to this figure, it takes much iteration to reach the steady state response. In this case, the response also has no overshoot.

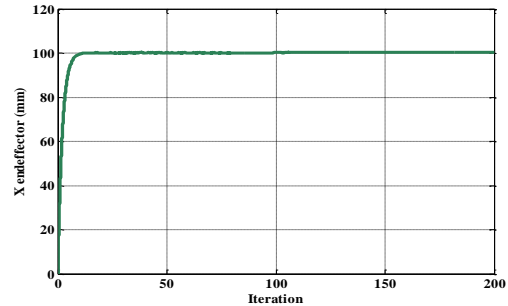


Fig 13. The controller response in X direction for a point in the trained workspace

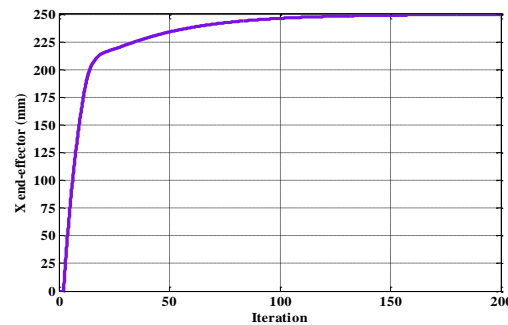


Fig 14. The controller response in X direction for a position far from the trained workspace

Comparing the results, shows that for the first case, the steady state of the system is approached in about 10 iteration, however, in the second case, the steady state is not reached completely even after 200 iteration, so, it can be concluded that the performance of the controller for the points near to the trained positions is much better, therefore, it is better to collect more data for training the robot and covers all the admissible workspace of the

robot. Although it takes more time, but, once the system is trained, and the model of the system is extracted, no additional time is required and the control can be done in real-time.

## 5. Conclusions

In this paper, first the structure of the robot, which constructed in the laboratory, was demonstrated and its actuation and sensory system that were required for data acquisition was explained. Then, the actuation signals and data acquisition procedure was represented. After that, due to the complexity of the dynamic model of the robot, system identification method was used instead of mathematical modeling of the robot. The obtained three-dimensional dynamic model was validated through the experimental results. Then this dynamic model obtained from system identification method, which captures the whole dynamic of the system was used for control purpose, it's worth to mention that this scheme is capable to be implemented in real-time, due to the simplicity and on-line estimation of the model, which is hardly achieved in mathematical dynamic models, because their closed-form solutions are time consuming. The PID-fuzzy system was used for controlling the system, because it was a model-less controller and does not require the exact model of the system and can be linked to the SI model. Finally, the performance of the system for reaching the points near the trained data and far from these data was compared and it was found that the performance of the controller is much better near the trained data.

## References

- [1] R. J. Webster III and B. A. Jones, "Design and kinematic modeling of constant curvature continuum robots: A review," *Int. J. Rob. Res.*, vol. 29, no. 13, pp. 1661–1683, 2010.
- [2] P. K. Singh and C. M. Krishna, "Continuum arm robotic manipulator: A review," *Univers. J. Mech. Eng.*, vol. 2, no. 6, pp. 193–198, 2014.
- [3] H. Yuan and Z. Li, "Workspace analysis of cable-driven continuum manipulators based on static model," *Robot. Comput. Integr. Manuf.*, vol. 49, pp. 240–252, 2018.
- [4] T. Kato, I. Okumura, H. Kose, K. Takagi, and N. Hata, "Tendon-driven continuum robot for neuroendoscopy: validation of extended kinematic mapping for hysteresis operation," *Int. J. Comput. Assist. Radiol. Surg.*, vol. 11, no. 4, pp. 589–602, 2016.
- [5] M. Calisti *et al.*, "Design and development of a soft robot with crawling and grasping capabilities," in *Robotics and Automation (ICRA), 2012 IEEE International Conference on*, 2012, pp. 4950–4955.
- [6] J. S. Mehling, M. A. Diftler, M. Chu, and M. Valvo, "A minimally invasive tendril robot for in-space inspection," in *The First IEEE/RAS-EMBS International Conference on Biomedical Robotics and Biomechatronics, 2006. BioRob 2006.*, 2006, pp. 690–695.
- [7] I. D. Walker, "Continuous backbone 'continuum' robot manipulators," *Isrn Robot.*, vol. 2013, 2013.
- [8] M. W. Hannan and I. D. Walker, "Analysis and experiments with an elephant's trunk robot," *Adv. Robot.*, vol. 15, no. 8, pp. 847–858, 2001.
- [9] M. W. Hannan and I. D. Walker, "Kinematics and the implementation of an elephant's trunk manipulator and other continuum style robots," *J. Robot. Syst.*, vol. 20, no. 2, pp. 45–63, 2003.
- [10] M. Dehghani and S. A. A. Moosavian, "Modeling and control of a planar continuum robot," in *Advanced Intelligent Mechatronics (AIM), 2011 IEEE/ASME International Conference on*, 2011, pp. 966–971.
- [11] M. C. Yip and D. B. Camarillo, "Model-less feedback control of continuum manipulators in constrained environments," *IEEE Trans. Robot.*, vol. 30, no. 4, pp. 880–889, 2014.
- [12] F. Renda, V. Cacucciolo, J. Dias, and L. Seneviratne, "Discrete Cosserat approach for soft robot dynamics: A new piece-wise constant strain model with torsion and shears," in *Intelligent Robots and Systems (IROS), 2016 IEEE/RSJ International Conference on*, 2016, pp. 5495–5502.
- [13] A. D. Kapadia, K. E. Fry, and I. D. Walker, "Empirical investigation of closed-loop control of extensible continuum manipulators," in *Intelligent Robots and Systems (IROS 2014), 2014 IEEE/RSJ International Conference on*, 2014, pp. 329–335.
- [14] T. George Thuruthel, Y. Ansari, E. Falotico, and C. Laschi, "Control Strategies for Soft Robotic Manipulators: A Survey," *Soft Robot.*, vol. 5, no. 2, pp. 149–163, 2018.
- [15] D. B. Camarillo, C. R. Carlson, and J. K. Salisbury, "Task-space control of continuum manipulators with coupled tendon drive," in *Experimental Robotics*, 2009, pp. 271–280.
- [16] A. Bajo, R. E. Goldman, and N. Simaan, "Configuration and joint feedback for enhanced performance of multi-segment continuum robots," in *Robotics and Automation (ICRA), 2011 IEEE International Conference on*, 2011, pp. 2905–2912.
- [17] M. Li, R. Kang, S. Geng, and E. Guglielmino, "Design and control of a tendon-driven continuum robot," *Trans. Inst. Meas. Control*, vol. 40, no. 11, pp. 3263–3272, 2018.
- [18] M. C. Yip and D. B. Camarillo, "Model-less hybrid position/force control: a minimalist approach for continuum manipulators in unknown, constrained environments," *IEEE Robot. Autom. Lett.*, vol. 1, no. 2, pp. 844–851, 2016.
- [19] A. Melingui, R. Merzouki, J. B. Mbede, C. Escande, B. Daachi, and N. Benoudjit, "Qualitative approach for inverse kinematic modeling of a compact bionic handling assistant trunk," in *Neural Networks (IJCNN), 2014 International Joint Conference on*, 2014,

pp. 754–761.

- [20] A. Melingui, O. Lakhali, B. Daachi, J. B. Mbede, and R. Merzouki, “Adaptive neural network control of a compact bionic handling arm,” *IEEE/ASME Trans. Mechatronics*, vol. 20, no. 6, pp. 2862–2875, 2015.
- [21] A. Parvaresh, S. A. Moosavi, and S. A. A. Moosavian, “Identification and Position Control of a Continuum Robotic Arm,” in *International Conference on Robotics and Mechatronics*, 2017.

## Biography



**Aida Parvaresh** received her BS degree in 2011 From Tabriz University, and MS degree in 2013 from Tabriz University in Mechanical Engineering. She is currently a PhD student at the Mechanical Engineering Department of K. N. Toosi University of Technology. Her thesis subject is in the

areas of dynamics modeling, and control of continuum (soft) robotic arms with the emphasis on configuration control.



**S. Ali A. Moosavian** received his BS degree in 1986 from Sharif University of Technology and the MS degree in 1990 from Tarbiat Modares University (both in Tehran), and his PhD degree in 1996 from McGill University (Montreal, Canada), all in Mechanical Engineering.

He is with the Mechanical Engineering Department at K. N. Toosi University of Technology (Tehran) since 1997, currently as a Professor. He teaches courses in the areas of robotics, dynamics, automatic control, analysis and synthesis of mechanisms. His research interests are in the areas of dynamics modeling, and motion/impedance control of terrestrial and space robotic systems. He has published more than 300 articles in peer-reviewed journals and conference proceedings. He is one of the founders of the ARAS Research Center for Design, Manufacturing and Control of Robotic Systems, and Automatic Machineries, and is currently the Director of Center of Excellence in Robotics and Control. He is the general and scientific chair of the Annual International Conference on Robotics and Mechatronic (ICROM).